Rabi-like oscillations of an anharmonic oscillator: classical or quantum effect?

Julien Claudon, Alex Zazunov, Frank. W. J. Hekking, Olivier Buisson

Rabi-like oscillations of an anharmonic oscillator: classical or quantum effect?

J. Claudon, A. Zazunov, F. W. J. Hekking, and O. Buisson
Institut Néel-LPMMC, C.N.R.S.- Université Joseph Fourier, BP 166, 38042 Grenoble-cedex 9, France
(Dated: September 24, 2007)

We have observed Rabi-like oscillations in a current-biased dc SQUID presenting enhanced coherence times compared to our previous realization [1]. This Josephson device behaves as an anharmonic oscillator which can be driven into a coherent superposition of quantum states by resonant microwave (μw) flux pulses. At large μw amplitude, the superposition involves many levels, and the system behaves classically. When the amplitude is reduced, a crossover region is found between this classical dynamics and a quantum two-level behavior. This intermediate regime involves a few levels and is fully explained by a quantum model, whereas a classical approach fails to describe the experimental data.

PACS numbers: ...

It is well-known that the classical dynamics of an anharmonic oscillator driven by an external monochromatic force can exhibit very complex and rich behavior. Examples are nonlinear resonances, bistability oscillations, and chaotic dynamics[2, 3, 4, 5]. The quantum analysis of this behavior constitutes a challenging problem [6, 7, 8, 9]. One needs to have a well defined system that ideally can be tuned all the way from the classical to the quantum limit. Along this transition a probe is needed that reveals clear signatures of quantum phenomena which can be compared to their classical counterparts. In this context, a current-biased dc SQUID presents an easily tuneable anharmonicity, enabling to explore the dynamics between these two limits. Recently, Rabi-like oscillations, involving more than two energy levels, where observed in the dc SQUID [1]. These phenomena, a direct consequence of the oscillator non-linearity, were discussed first using a quantum analysis [1] and then using a classical approach [10]. This double interpretation opens the question whether Rabi-like oscillations are an unambiguous proof of quantum behaviour. In this letter, we report the measurement of Rabi-like oscillations in a new SQUID circuit for various μw amplitude. Improved coherence times with respect to previous experiments [1] enable us to explore the crossover from two-level to multilevel dynamics in detail. The experimental data exhibit a clear quantum behavior, which can definitely not be explained by a classical approach.

The anharmonic oscillator under consideration is realized in a current biased dc SQUID, which consists of two identical Josephson junctions (JJ), each with a critical current I_0 and a capacitance C_0. The junctions are embedded in a superconducting loop of total inductance L_s, threaded by a flux Φ_b. As discussed in Ref. [11], the phase dynamics of the SQUID can be treated as that of a fictitious particle having a mass $m = 2C_0(\Phi_0/2\pi)^2$ moving in a one-dimesional cubic potential ($\Phi_0 = h/2e$ is the superconducting flux quantum). The potential is completely characterized by the frequency ν_p of the bottom of the well and a barrier height ΔU [Fig. 1]. These two quantities depend on the magnetic flux and vanish at the SQUID's critical current I_c. For bias currents $I_b < I_c$,

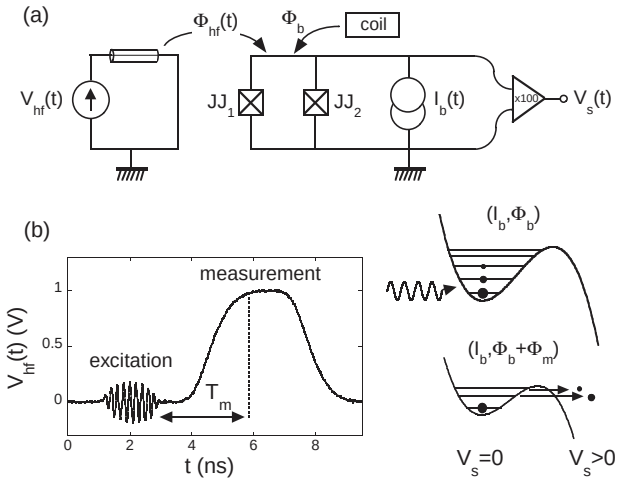

FIG. 1: Principle of the SQUID operation. (a) Schematic of the electrical circuit. (b) Digital sampling oscilloscope record of the high frequency flux signal applied on the superconducting loop: the μw excitation pulse is followed by a measuring dc pulse which adiabatically reduces the barrier height and induces a selective tunnel escape of excited states.

the particle is trapped in the anharmonic potential well. In presence of an applied driving magnetic flux, the corresponding Hamiltonian reads:

$$\hat{H}_0(t) = \frac{\hat{p}^2}{2m} + \frac{1}{2}m\omega_p^2\hat{x}^2 - a\hat{x}^3 + f_{\mu w}\cos(2\pi\nu t)\hat{x}\,. \quad (1)$$

Here, $\omega_p = 2\pi\nu_p$; $\hat{x}$ is the phase along the escape direction, and $\hat{p}$ is the conjugate momentum associated with the charge on the junction capacitance, $\hat{Q} = (2e/\hbar)\hat{p}$. The cubic coefficient is given by $a^2 = (m\omega_p^2)^3/(54\Delta U)$. The μw flux acts as an oscillating force with a strength $f_{\mu w}$ and a frequency ν. Starting from Eq. (1), the SQUID dynamics can be treated either classically or with quantum mechanics. In a quantum description and in the absence of driving flux signal, the quantized vibration states within the potential well are denoted $|n\rangle$, corresponding to energy levels E_n with $n = 0, 1, ...$ The frequency associated to the $|n\rangle \rightarrow |k\rangle$ transition is denoted ν_{nk}. The

parameter $\delta = \nu_{01} - \nu_{12}$ characterizes the system anharmonicity.

Our procedure to perform experiments consists of the repetition of an elementary sequence, which is decomposed into four successive steps. First, a bias current I_b is adiabatically switched on through the SQUID at fixed magnetic flux Φ_b. The working point (I_b, Φ_b) defines the geometry of the potential well and the circuit is initially in the ground state. A fast composite flux signal, presented in Fig. 1(b), is then applied. The μw excitation pulse is followed by a dc flux pulse which brings the system to the measuring point within a few nanoseconds. This flux pulse reduces adiabatically the barrier height ΔU and allows escape of the localised states to finite voltage states. Adjusting precisely the amplitude and duration of the dc flux pulse, it is theoretically possible to induce a selective escape of excited states. Because the SQUID is hysteretic, the zero and finite voltage states are stable and the result of the measurement can be readout by monitoring the voltage V_s across the dc SQUID. Our measurement procedure destroys the superconducting state and I_b has to be switched off to reset the circuit.

Though adiabatic, our measurement is one of the fastest implemented in Josephson qubits. The delay between the end of μw and the measurement (top of the dc pulse) is less than 3 ns. The measurement time, corresponding to the top of the pulse, is 4 ns. The measurement speed is crucial to efficiently detect fast relaxing states. This is especially true for a multilevel system, since the relaxation rate of the excited state $|n\rangle$ scales as n. Detection in the multilevel regime has been characterized in Ref. [12] for settings identical to those used in this article. For states described by the set of occupancies $\{p_0, p_1, p_2, p_3\}$, the escape probability P_e out of the potential well reads: $P_e = 0.03 + 0.54p_1 + 0.79p_2 + 0.90p_3$.

The SQUID studied in this article consists of two large JJs of 15 μm^2 area ($I_0 = 1.242\,\mu$A and $C_0 = 0.56$ pF) enclosing a 350 μm^2-area superconducting loop. The two SQUID branches of inductances L_1 and L_2 contribute to the total loop inductance $L_s = 280$ pH with the asymmetry parameter $\eta = (L_1 - L_2)/L_s = 0.414$. The chip is cooled down to 30 mK in a dilution fridge. Thermal energy is then small compared to the oscillation energy of the circuit $h\nu_p \sim k_B \times 500$ mK. The high frequency flux signal is guided by 50 Ω coax lines and attenuated at low temperature before reaching the SQUID through a mutual inductance. The nominal room temperature μw amplitude is denoted in the following $V_{\mu w}$. For details on the circuit fabrication and the experimental setup description, we refer to Ref. [12].

Hereafter we present results obtained at the working point ($I_b = 2.222\ \mu$A, $\Phi_b = -0.117\ \Phi_0$). The experimental low power spectroscopy measurements (Fig. 2(a)) present a resonant peak centred at 8.283 GHz with a full width at half maximum $\Delta\nu = 110$ MHz. The resonance is interpreted in a quantum description as the transition from $|0\rangle$ to $|1\rangle$ at the frequency ν_{01}. Having the SQUID electrical parameters in hand, the characteristics of the potential well are calculated. The plasma frequency is $\nu_p = 8.428$ GHz and the well contains 9 energy levels for a total depth $\Delta U = h \times 71.1$ GHz. The three higher energy levels in the well have tunnel lifetime smaller than 50 μs, the duration of current biasing. Only the lower levels which are stable on the time scale of the experiment are concerned here. Compared to Ref. [1], the present sample has lower decoherence ($\Delta\nu = 110$ MHz instead of 180 MHz), and the chosen bias point displays higher anharmonicity ($\delta = 160$ MHz instead of 100 MHz). This improvement allows for much more transition selective coherent μw driving.

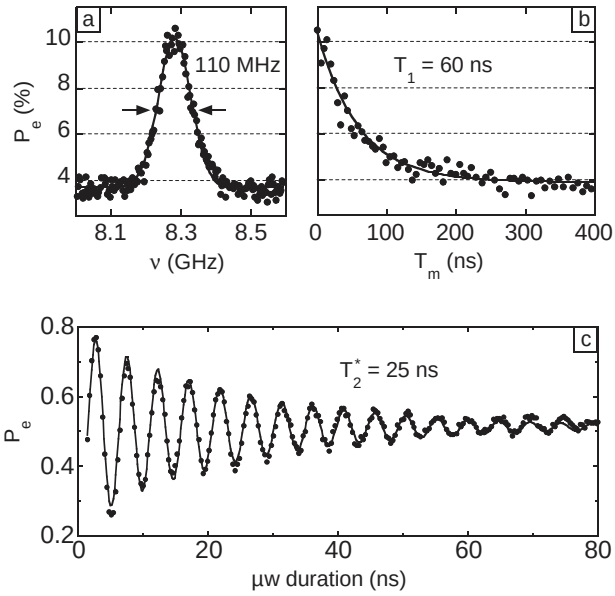

FIG. 2: (a): low power spectroscopy ($V_{\mu w} = 17.8$ mV). The fit to a Gaussian lineshape gives the resonance position and the linewidth. (b): energy relaxation as a function of the measurement delay T_m, fitted to an exponential law with the damping time T_1. (c): Rabi-like oscillation observed in the transient regime for high power μw driving ($V_{\mu w} = 631$ mV). The oscillation frequency and the damping time T_2^* are extracted from a fit to an exponentially damped sine function.

The transient non linear dynamics of the SQUID is probed using a fast μw flux pulse followed by a measuring dc pulse. The μw excitation is tuned on the resonance frequency (8.283 GHz) and the μw pulse duration is increased from 2 ns to 80 ns. The measurement delay, as well as the other measurement pulse settings, remain unchanged. During the transient regime, Rabi like oscillations (RLO) are observed. From a fit of the first oscillations to a damped sine function, the RLO frequency ν_{RLO} and the damping characteristic time T_2^* are extracted. For the oscillation plotted in Fig.2(c), T_2^* reaches 25 ns, confirming the coherence improvement in this sample. In the following, we foccus on the dependence of ν_{RLO} with the μw amplitude. The issue addressed in the article is whether this particular measurement offers a clear signature of quantum behaviour, or not.

We first apply the classical approach developed in

Ref. [10]. Having turned on the resonant driving force, the particle energy oscillates during a transient regime. The underlying mechanism is related to the potential non-linearity, which induces a dephasing between the particle oscillations and the μw excitation. It makes the μw alternatively accelerate and brake the particle oscillations within the well. For consistency, we should note that, in a classical description, the low power resonance presented in Fig. 2(a) is associated with the plasma frequency characterizing the bottom of the well. As spectroscopic data are used to extract the SQUID parameters, the classical analysis leads to slightly different electrical parameters; they are listed in note [13]. Fig. 3(a) shows the fit of experimental data to the classical theory. The calibration coefficient between the applied μw amplitude and $f_{\mu w}$ is the only free parameter of the model. When losses are neglected or very small to be consistent with the measured $T_1 = 60\,\text{ns}$ time (Fig. 2(b), see Ref. [14] for measurement description), the model predicts a $f_{\mu w}^{2/3}$ law which is strongly different from the observed linear dependence at low μw amplitude. However, the agreement improves for higher driving amplitude. As a remark, we can note that the ν_{RLO} versus $f_{\mu w}$ dependence can be perfectly fitted with $T_1 = 2.5\text{ns}$. However, with such an excessive dissipation, Rabi like oscillations are overdamped with a damping time about 3ns (Fig. 3(c)) which is one order of magnitude smaller than the measured one. This hypothesis is inconsistent with experimental observations and is therefore discarded.

The explanation of experimental data requires a full quantum treatment. We first develop a pure Hamiltonian approach similar to Ref. [1], neglecting all decoherence sources. The well is assumed to be initially in the ground state. At $t = 0$, the μw flux is switched on, and the quantum state of the well evolves into a superposition of the level states, $|\Psi(t)\rangle = \sum_n A_n(t)|n\rangle$, with amplitudes $A_n(t)$ satisfying the Schrodinger equation with the Hamiltonian (1): $i\hbar\partial_t A_n = E_n A_n + \sqrt{2}\hbar\,\Omega_1\cos(\omega t)\sum_k X_{nk}\,A_k$, where $\omega = 2\pi\nu$, $X_{nk} = \sqrt{m\omega_p/\hbar}\langle n|\hat{x}|k\rangle$ and $\Omega_1 = f_{\mu w}/\sqrt{2m\hbar\omega_p}$ is the Rabi angular frequency in the two-level system represented by the two lowest levels of the well. In the Rotating Wave Approximation (RWA), the amplitudes are given by $A_n(t) = e^{-i(n\omega+\lambda_n)t}\,a_n$, where λ_n and a_n are obtained by solving the following eigenvalue system:

$$\lambda_n a_n = \epsilon_n a_n + \frac{\Omega_1}{\sqrt{2}}\left(X_{n,n+1}\,a_{n+1} + X_{n,n-1}\,a_{n-1}\right)\,, \quad (2)$$

with $\epsilon_n = \left(E_n - n\hbar\omega\right)/\hbar$. As shown in Fig. 4(b), the average energy of the particle undergoes Rabi like oscillations. In addition, beating effects are also predicted: they will be discussed in the end of the article. To extract the theoretical Rabi-like oscillations frequencies, the first oscillations obtained numerically are fitted by an exponential damped sine function.

As shown in Fig. 4(a), the quantum model describes all the experimental features of the ν_{RLO} versus Ω_1 dependence. Again, the only free parameter of the fit is the

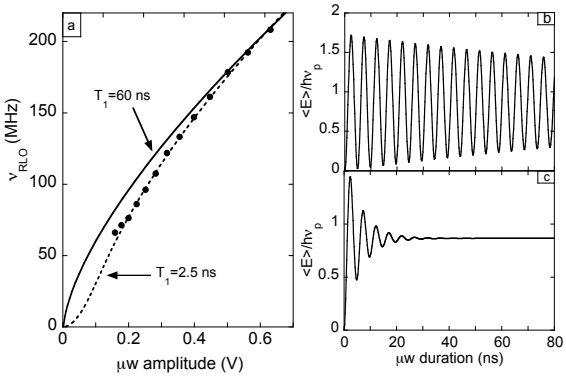

FIG. 3: Classical description of Rabi-like oscillations. (a): Best fit of the experimental ν_{RLO} (•) to the classical theory with losses consistent with measurement (solid line). The classical model fails to describe the low amplitude regime. Introducing arbitrary high losses, it is possible to reproduce experimental data (dashed line). However, this T_1 is not consistent with energy relaxation measurement and leads to overdamped Rabi-like oscillations (c) which are not consistent with the measured T_2^*. On the right: calculated mean energy of the particle versus the μw duration with $T_1 = 60\,\text{ns}$ (b) and $T_1 = 2.5\,\text{ns}$ (c), for a μw amplitude corresponding to Fig. 2(c).

calibration coefficient between the applied μw amplitude and Ω_1. The set of experimental data covers the crossover between the 2-level and the multilevel dynamics. Indeed, when the μw amplitude is small compared to the anharmonicity ($\Omega_1/2\pi \ll \delta$), the dynamics concerns mainly the two first level and one retreives the familiar result $\nu_{RL0} = \Omega_1/2\pi$. This is practically the case for the first measured point, which corresponds to $\Omega_1/2\pi = 65\,\text{MHz}$. The calculated contamination of level $|2\rangle$ during the oscillation is then lower than 12 %. For $\Omega_1/2\pi \sim \delta$, 3 levels are involved in the dynamics. Surprisingly, the ν_{RL0} dependence on Ω_1 remains roughly linear. When $\Omega_1/2\pi > \delta$, an increasing number of level are involved. As an example, the experimental oscillation presented in Fig. 2(c) involves 4 states. At larger μw amplitude, a macroscopic number of levels are involved. This regime is not achieved at this working point but was discussed in Ref. [1] with about ten levels involved. The multilevel dynamics is characterised by a clear saturation of the ν_{RLO} dependence, compared to the low Ω_1 linear behaviour.

Interestingly, the classical and the quantum approach give a very similar result for $\Omega_1/2\pi > \delta$. However, for the lowest μw amplitude in this range, 4 states are involved in the dynamics. Under these conditions, the energy granularity is significant compared to the mean energy in the system. To proceed, we may draw a parallel with the coherent states which build up in an harmonic oscillator driven by μw. Except for zero point fluctuations, these states rigorously follow classical mechanics. In an anharmonic system, non linearity induces RLO. There is a clear quantum signature in the ν_{RLO} versus Ω_1 depen-

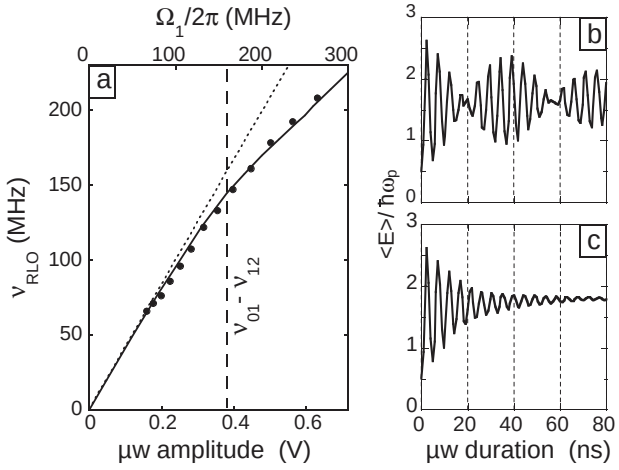

FIG. 4: Quantum description of Rabi-like oscillations. (a) Fit of the experimental ν_{RLO} (•) to the quantum theory (solid line). For $\Omega_1/2\pi > \nu_{01} - \nu_{02}$, the curve deviates from the two level theory (dashed line), indicating a multilevel dynamics. On the right: calculated mean energy of the particle versus the μw duration, without (a) and with decoherence (b) for $\Omega_1/2\pi = 260$ MHz (μw amplitude corresponding to Fig. 2(c)).

dence when $\Omega_1/2\pi < \delta$. This quantum signature disappears for higher μw amplitudes. Indeed for higher driving amplitudes, the system only feels the non-linearity of the potential when its energy is maximum. This explanation is supported by wave-function calculations: except near mean energy maxima, the wave function $\langle X|\Psi(t)\rangle$ describing the fictitious particle in the phase (X) representation is nearly Gaussian, as for a coherent state.

In the absence of dissipation, the quantum model predicts a beating in the Rabi-like oscillations. This effect should become more pronounced with increasing μw amplitude, that is, when the third and higher levels get involved. The predicted coherent beating has not been observed in our experiment. We have first analyzed the possibility of beating suppression caused by the finite rise time of the μw amplitude (up to 2 ns). We found that this effect does not lead to destructive interference strong enough to suppress the beating. We therefore argue that the strong suppression of the beating phenomenon could be due to decoherence. To analyze this, we have studied the dissipative dynamics of the well using a phenomenological, minimal model. We assume that the reduced density matrix of the driven oscillator satisfies the master equation

$$i\hbar\partial_t\rho = [H_{RWA}, \rho] - i\mathcal{L}_R[\rho] - i\mathcal{L}_D[\rho]\,. \qquad (3)$$

Here H_{RWA} is the RWA Hamiltonian in the rotated basis corresponding to Eq. (2) and $\mathcal{L}_{\mathcal{R}}[\rho]_{kn} = \sum_m [(\gamma_{km} + \gamma_{nm})\,\rho_{kn} - 2\delta_{kn}\gamma_{mk}\rho_{mm}]$ describes relaxation (accompanied by dephasing). The coefficients γ_{kn} can be calculated microscopically in the Markovian limit assuming the environment to be a bath of harmonic oscillators. The last term, $\mathcal{L}_{\mathcal{D}}[\rho]_{kn} = (1-\delta_{kn})\Lambda_{kn}\rho_{kn}$ with $\Lambda_{kn} = \Lambda_{nk} \geq 0$, describes the pure dephasing. This term is phenomenological: the coefficients Λ have been obtained microscopically only in the two-level limit. According to our analysis, relaxation alone (corresponding to $T_1 = 60$ ns in the experiment) is too weak to explain a strong suppression of the beating. Instead, the absence of beating can be attributed to strong pure dephasing between next-neighboring levels, described by $\Lambda_{n,n+2}$. Indeed, the observed exponential decay of the Rabi-like oscillations with the suppressed beating can be well explained assuming $\Lambda_{02} \approx \alpha/\Omega_1$, which becomes relevant for the measured escape probabilities corresponding to the cases of $\Omega_1/2\pi = 130$ and 260 MHz with $\alpha = 31\,10^6\,h\times$ GHz rad/s.

In conclusion, a dc SQUID is a tunable and well defined anharmonic quantum oscillator which appears as an experimental model system to explore quantum and classical dynamics. The dependence of the Rabi-like oscillation frequency on the μw amplitude is a clear probe of the nature of oscillator dynamics. When the μw amplitude is small enough to involve only a few levels, the dependence exhibits clear quantum behavior which is not described by a classical model. The shape of the oscillations contains more informations on the multilevel dynamics which will be studied in the future.

We thank F. Faure, W. Guichard, L. P. Lévy, and A. Ratchov for fruitfull discussions. This work was supported by two ACI programs, by IUF and IPMC and by the EuroSQIP project.

[1] J. Claudon, F. Balestro, F. W. J. Hekking, and O. Buisson, Phys. Rev. Lett. **93**, 187003 (2004).
[2] L. D. Landau and E. M. Lifshitz, Mechanics (Pergamon Press, NewYork, 1976), 3rd ed.
[3] P.S. Linsay, Phys. Rev. Lett. **47**, 1349 (1981).
[4] A. Barone and G. Paterno, *Physics and Applications of the Josephson Effect* (Wiley, New York, 1982); K. K. Likharev, *Dynamics of Josephson Junctions and Circuits* (Gordon and Breach, New York, 1986).
[5] I. Siddiqi et al, Phys. Rev. Lett. **93**, 207002 (2004).
[6] *Dissipative Systems in Quantum Optics*, Vol. 27 of Topics in Current Physics, edited by R. Bonifacio (Spinger, Berlin, 1982).
[7] G. J. Milburn, Phys. Rev. A **33**, 674 (1986).
[8] *Quantum Chaos: Proceedings of the Adriatico Research Conference on Quantum Chaos* , edited by H. A. Cerdeira et al. (World Scientific, Singapore, 1991);
[9] D. Enzer and G. Gabrielse, Phys. Rev. Lett. **78**, 1211 (1997).
[10] N. Gronbech-Jensen and M. Cirillo, Phys. Rev. Lett. **95**, 067001 (2005); J. E. Marchese, M. Cirillo and N. Gronbech-Jensen, Phys. Rev. B **73**, 174507 (2006).

[11] F. Balestro, J. Claudon, J. Pekola, and O. Buisson, Phys. Rev. Lett. **91**, 158301 (2003).
[12] J. Claudon, A. Fay, E. Hoskinson, and O. Buisson, cond-mat/0702453 (2007), accepted at Phys. Rev. B.
[13] Parameters for the classical analysis: $C_0 = 0.58\,\mathrm{pF}$, $\nu_p = 8.283\,\mathrm{GHz}$ and $\Delta U = 69.9\,h\times$ GHz.
[14] J. Claudon, A. Fay, L. P. Lévy, and O. Buisson, Phys. Rev. B **73**, 180502(R) (2006).